

# A combined fit to the Higgs Branching Ratios at ILD

Jonas Kunath\*, Fabricio Jimenez Morales, Jean-Claude Brient, and  
Vincent Boudry

Laboratoire Leprince-Ringuet CNRS, École Polytechnique,  
Institut Polytechnique de Paris, France

Higgs decay branching ratios at future Higgs factories can be measured by directly exploiting class numeration. Given the clean environment at a lepton collider, it is possible to build an event sample highly enriched in Higgs bosons and essentially unbiased for any decay mode. The sample can be partitioned into categories using event properties linked to the expected Higgs decay modes. The counts per category are used to fit the Higgs branching ratios in a model independent way. The result of the fit is the set of branching ratios, independent from a Higgs production mode measurement.

We present a simplified study on simulated data for the International Linear Detector (ILD) at the International Linear Collider (ILC) at 250 GeV center-of-mass energy.

## 1 Introduction

The ILC as a Higgs factory will produce a large number of Higgs bosons in the comparatively simple collision environment of a lepton collider. The projected gain on the precision of Higgs measurements will make them sensitive to deviations that are predicted by theories of physics beyond the Standard Model (BSM).

With the Higgsstrahlung process at a Higgs factory it is possible to construct an unbiased sample in which each type of Higgs decay occurs with the probability given by its branching ratio (BR) realized in nature [1]. Higgsstrahlung events with  $Z \rightarrow e^+e^-$  and  $Z \rightarrow \mu^+\mu^-$  can be selected by reconstruction of the primary  $Z$  boson, independently of the Higgs decay [2].

Figure 1 shows how such a sample can be partitioned into a number of classes with each of the class selection efficiencies depending on the specific Higgs decay mode. The relative frequency of the number of events per class depends on the Higgs BRs. An inclusive estimation of all branching ratios can be obtained through a fit on the class counts. The

---

\*Presenter. Talk presented at the International Workshop on Future Linear Colliders (LCWS2021), 15-18 March 2021. C21-03-15.1

approach naturally lends itself to an extension with additional classes which target BSM Higgs decays. Additional decay modes can thus be excluded with an upper limit that depends on the sample size.

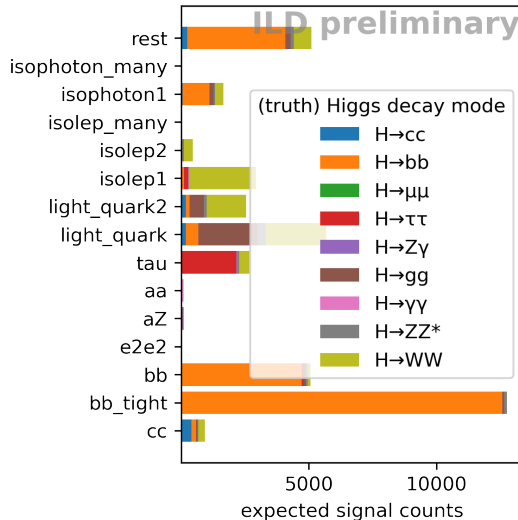


Figure 1: Expected contributions per class from each of the Higgs decay modes assuming the Standard Model branching ratios. The class definitions are listed in the appendix.

The presented study is realized in the context of the International Linear Detector (ILD) [3, 4]. The ILD detector concept is proposed for the International Linear Collider (ILC). The detector design is based on the particle flow approach for particle reconstruction [5]. Only running scenarios of the ILC with a center-of-mass energy of  $\sqrt{s} = 250$  GeV (ILC250) are considered here.

The fit is in a preliminary state. The simulation procedure is described in Section 2, a summary of the current simplifications in 2.1. Preliminary results from the fit, with some known shortcomings, are already available. They are given in Section 3. An outline of the necessary future work is presented in Section 4. Finally, the note is summarized in Section 5.

## 2 Simulation

We use samples produced by the ILD concept group since 2020. They are obtained from a detailed simulation of the ILC250 with the new SetA beam parameters [6].

The events are generated at leading order using WHIZARD version 2.8.5 [7, 8]. Initial State Radiation, Beamstrahlung and Final State Radiation are included. The fragmentation and hadronization of final-state quarks and gluons is performed with PYTHIA 6.422 [9]. The ILD detector geometry is described with DD4hep [10] and simulated in GEANT4 [11]. Event reconstruction is performed with ILCSoft v02-02 [12], which includes PandoraPFA [13] for the construction of particle flow objects and LCFIPlus [14] for flavor tagging.

As the simulated data set is used for two different tasks, it is split into two equal but statistically independent parts. The first part of the available data (MC1) is needed to set up the fit of BRs. The second part (MC2) is used to generate the counts per class. This second part serves as a placeholder for the detector data. Having MC2 as a separate

sample is required for being able to evaluate the bias that the method has due to the limited size of MC1. By changing the BRs in MC2, through changing the event weights, the adaptability of the fit is validated. This is illustrated in Figure 3.

## 2.1 Current simplifications

Results shown here are obtained without considering background processes. As signal channel,  $\nu\bar{\nu}H$  is used without a pre-selection step for background reduction. While it is not a realistic scenario, this pure-Higgs sample can provide a first idea of the precision and adaptability of the method.

For each of the nine considered main BRs of the Higgs boson, at least 400k simulated events are used. They are separately weighted and combined into a single sample with exactly 40k signal Higgs events. Different Higgs BR scenarios are tested by changing the weights.

Note that 40k Higgs events corresponds to about 10% of the Higgs bosons produced in the long-running H-20 scenario of the ILC250 [15]. Even before taking into account selection inefficiencies, only less than 7% of the produced Higgs bosons are in the  $Z \rightarrow e^+e^-$  and  $Z \rightarrow \mu^+\mu^-$  samples combined. As mentioned in Section 4 we expect to be able to leverage the  $\nu\bar{\nu}H$  sample. Future work will have to show if a 10% sample size is a good estimation of the gain from the  $\nu\bar{\nu}H$  sample.

## 3 Branching ratio uncertainties

For each Higgs decay mode, a probability vector is constructed from the simulation (MC1). This vector stores the selection efficiency and the probabilities for the events of the chosen type to belong to each of the classes that are constructed within the sample. The vectors can be collected as columns into a probability matrix  $M$ . Data counts are generated from the test sample (MC2) as placeholders for future detector data.

A fit is then performed with `iminuit` [16, 17]. The Standard Model (SM) Higgs branching ratios (BRs) are taken as the starting values of the fit. Based on a multinomial log-likelihood as its cost function, the 9 considered independent BRs of the Higgs boson are described through 8 parameters in the fit. We obtain a prediction for the 8 parameters and the corresponding covariance matrix. From those we get the mean values and uncertainties of the BRs.

The result of this fit is shown in Figure 2 for the SM BRs and an alternative scenario. To have a change that can be comfortably spotted by eye, the alternative scenario has the  $BR(H \rightarrow b\bar{b})$  decreased by 15%, which is fully compensated by  $BR(H \rightarrow W^+W^-)$ . Since the probability vectors of the decay modes are different enough, the fit moves to the altered BRs without any problems. The fit not landing at the altered BRs would have suggested that the defined classes do not have sufficient discriminating power between some of the BRs.

The uncertainties on the BRs can be tested in a toy study. The uncertainties and correlations of the fit on the expected event counts are obtained through the second derivatives of the likelihood function at the fit optimum. For the toy study, samples are drawn from a multinomial distribution centered on the expected counts for each class. Then, a fit is performed for each of the samples, and the predicted branching ratio optima are collected. An example toy study on the  $H \rightarrow b\bar{b}$  branching ratio is shown in Figure 3. The dotted grey line indicates the SM value of the  $H \rightarrow b\bar{b}$  coupling in the simulation. The black line

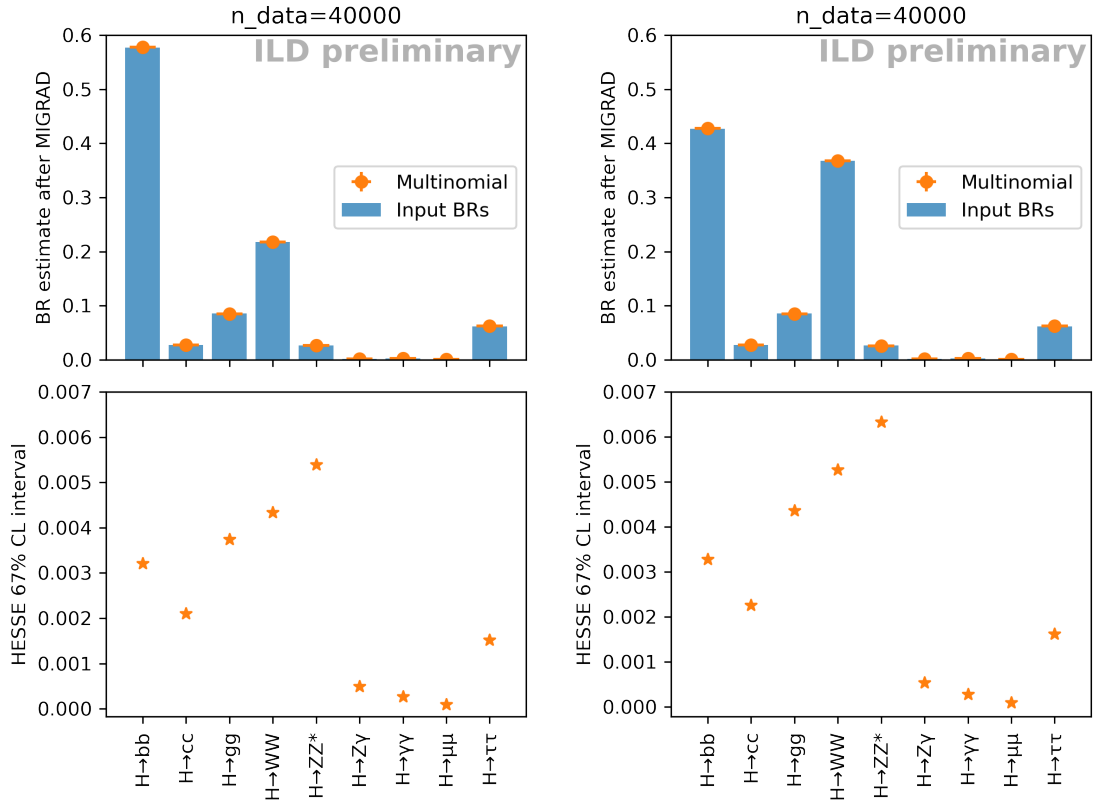


Figure 2: Top row: Branching ratios assumed for the generation of the counts per class. Fit optimum and its uncertainty are given as orange error bars. The starting values of the fit are always the SM Higgs BRs. The considered scenarios are the SM BRs (left) and a BSM scenario described in the text.

Bottom row: The absolute statistical uncertainties of the fit per branching ratio.

indicates the optimum of a fit on the expected event counts. It was validated that the difference between these two lines is only due to limited Monte Carlo statistics. The blue Gaussian curve has as standard deviation the uncertainty of the fit on the expected event counts, as quoted by MINUIT. The orange histogram contains the fit optima from 10k fits on event counts varied according to a multinomial distribution centered on the expected event counts. The values from the toy study agree well with those anticipated from the fit of the expected event counts.

The projected (absolute)  $1\sigma$ -uncertainties for the Higgs branching ratios are listed in Table 1 and illustrated in Figure 2 (bottom row). The numbers are based on the simplified scenario outlined in Section 2.1.

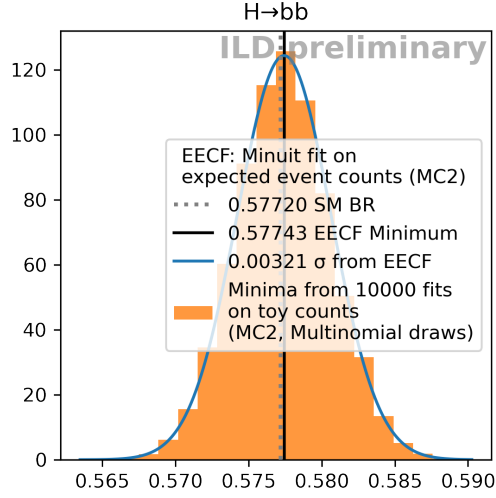


Figure 3: Validation of the uncertainty from a fit on the expected event counts scenario against a toy study.

|                              | SM BR  | fitted BR | $\sigma_{\text{stat}}$ |
|------------------------------|--------|-----------|------------------------|
| $H \rightarrow cc$           | 2.718  | 2.733     | 0.210                  |
| $H \rightarrow bb$           | 57.720 | 57.743    | 0.321                  |
| $H \rightarrow \mu\mu$       | 0.030  | 0.030     | 0.009                  |
| $H \rightarrow \tau\tau$     | 6.198  | 6.207     | 0.152                  |
| $H \rightarrow Z\gamma$      | 0.170  | 0.176     | 0.050                  |
| $H \rightarrow gg$           | 8.550  | 8.499     | 0.374                  |
| $H \rightarrow \gamma\gamma$ | 0.242  | 0.243     | 0.027                  |
| $H \rightarrow WW$           | 21.756 | 21.761    | 0.434                  |
| $H \rightarrow ZZ^*$         | 2.616  | 2.608     | 0.539                  |

Table 1: Preliminary results of a MINUIT fit on the expected event counts. The table gives fitted values of the Higgs BRs and their absolute statistical uncertainties. All numbers are given in percent.

## 4 Future work

The next iteration of this study has to include the background rates for Higgs-free events passing the selection. Then, the proper cross sections and the polarizations foreseen at ILC can be applied.

In the  $\nu\bar{\nu}H$  sample it is not possible to perform an event selection which is independent of the Higgs decay products. Thus, this sample alone cannot be used for a branching ratio derivation with an unconditional upper limit on the unobserved branching ratio. But in combination with the other samples, the larger statistics of this sample should help decrease the uncertainties. The  $\nu\bar{\nu}H$  sample should be added to the combined fit, after choosing a good pre-selection.

The decay products from the  $Z \rightarrow e^+e^-$  and  $Z \rightarrow \mu^+\mu^-$  decays of the primary  $Z$  boson in a Higgsstrahlung event can be reliably identified. They can be separated from the rest of the event and exploited for the event selection. Since the identification of all particles from  $Z \rightarrow \tau^+\tau^-$  or  $Z \rightarrow q\bar{q}$  decays can be more complicated it is not planned to use those Higgsstrahlung events.

The current class definitions are listed in the appendix. They are only an initial draft with potential for improvement. The rest class should be reserved almost exclusively for background (or unexpected Higgs decay) events. For some of the Higgs decays, including  $H \rightarrow W^+W^-$ , no proper classes are designed yet.

A mechanism that indicates the case of non-SM Higgs decays ( $H \rightarrow \mu^+\tau^-$ ,  $H \rightarrow b\bar{c}$ , ...) has to be established. This could be through one or more additional classes or through a comparison of the value of the likelihood at the fit minimum with the likelihood minimum for the expected class counts.

## 5 Conclusion

An simultaneous measurement of all the Higgs branching ratios at once is an appealing objective. It can give upper limits for unobserved Higgs decays. The measurements of the individual branching ratios are connected through the covariance matrix of the fit. The preliminary results are attractive and motivate improvements towards a more realistic analysis.

## Acknowledgements

The authors would like to thank the LCC generator working group and the ILD software working group for providing the simulation and reconstruction tools and producing the Monte Carlo samples used in this study. This work has benefited from computing services provided by the ILC Virtual Organization, supported by the national resource providers of the EGI Federation and the Open Science GRID.

## References

- [1] J.-C. Brient, “A method to improve the precision of the branching fraction measurements of all Higgs decays” Talk at LCWS2019.
- [2] J. Yan, K. Fujii, J. Tian, “Model independence of the measurement of the  $e^+e^- \rightarrow ZH$  cross section using  $Z \rightarrow \mu^+\mu^-$  and  $Z \rightarrow e^+e^-$  at the ILC” arXiv:1601.06481 (2016).
- [3] H. Abramowicz et al., “The International Linear Collider Technical Design Report - Volume 4: Detectors”, arXiv:1306.6329 (2013).
- [4] The ILD Collaboration, “International Large Detector: Interim Design Report”, arXiv:2003.01116 (2020).
- [5] J.-C. Brient, H. Videau, “The Calorimetry at the future  $e^+e^-$  linear collider”, arXiv:hep-ex/0202004 (2002).
- [6] L. Evans, S. Michizono, “The International Linear Collider Machine Staging Report 2017”, arXiv:1711.00568 (2017).
- [7] W. Kilian, T. Ohl, J. Reuter, “WHIZARD: Simulating Multi-Particle Processes at LHC and ILC”, Eur. Phys. J. C 71 1742 (2011).
- [8] M. Moretti, T. Ohl, J. Reuter, “O’Mega: An Optimizing matrix element generator”, arXiv:hep-ph/0102195 (2001).
- [9] T. Sjostrand, S. Mrenna, P. Skands, “Pythia 6.4 physics and manual”, arXiv:hep-ph/0603175 (2006).
- [10] M. Frank, F. Gaede, M. Petric., “AIDASoft/DD4hep”, DOI: 10.5281/zenodo.4638724 (2021).
- [11] S. Agostinelli, et. al., “GEANT4—a simulation toolkit”, Phys. Res., Sect. A 506, 250 (2003).
- [12] <http://ilcsoft.desy.de/portal/> (2021).
- [13] M. Thomson, “Particle Flow Calorimetry and the PandoraPFA Algorithm”, Nucl. Instrum. Meth. A 611, 25 (2009).
- [14] T. Suehara, T. Tanabe, “LCFIPlus: A Framework for Jet Analysis in Linear Collider Studies”, Nucl. Instrum. Meth. A808 109–116 (2016).
- [15] T. Barklow et. al., “ILC Operating Scenarios”, arXiv:1506.07830 (2015).
- [16] F. Fames, M. Roos, “Minuit – A System for Function Minimization and Analysis of the Parameter Errors and Correlations” DOI: 10.1016/0010-4655(75)90039-9 (1975).
- [17] H. Dembinski, P. Ongmongkolkul et al., “scikit-hep/iminuit” DOI: 10.5281/zenodo.4310361 (2021).

# Appendix

## Class definitions

The current class definitions are only an initial attempt. They will be refined and extended.

An event belongs to the first class for which it passes the selection. The class selections are applied in the order listed below. It is not necessary that a class has a high purity for a specific branching ratio. The relative contributions that are expected from the Higgs decay modes for each of the classes should be disparate.

All variables are built exclusively on the Higgs-candidate part of the event excluding isolated leptons and final state radiation photons from the primary Z boson decay. Isolated leptons and isolated photons are identified through the IsolatedLeptonTaggingProcessor and IsolatedPhotonTaggingProcessor [12].

The flavor tagging is performed after forcing the (Higgs part of the) event into two jets. Through LCFIPlus [14] we obtain a score for b-likeness (*btag*) and for c-likeness (*ctag*) for each of the two jets. Each score lies between 0 and 1. Their sum cannot exceed 1. The sum is small when the jet is identified as likely stemming from a light quark.

1. **cc**: Targets  $H \rightarrow c\bar{c}$ :
  - No isolated leptons or photons.
  - $M_H > 100$  GeV.
  - More than 20 Particle Flow Objects (PFOs).
  - $ctag1 > 0.5, ctag2 > 0.5$ .
2. **bb\_tight**: Targets  $H \rightarrow b\bar{b}$ :
  - No isolated leptons or photons.
  - $btag1 > 0.8, btag2 > 0.8$ .
3. **bb**: Also targets  $H \rightarrow b\bar{b}$ :
  - No isolated leptons or photons.
  - $btag1 > 0.8$ .
4. **e2e2**: Targets  $H \rightarrow \mu^+\mu^-$ :
  - Has an opposite-charge pair of isolated muons.
  - $M_{\mu^+\mu^-} \in [100 \text{ GeV}, 130 \text{ GeV}]$ .
5. **aZ**: Targets  $H \rightarrow \gamma Z$ :
  - Has an isolated photon.
  - $M_\gamma \in [20 \text{ GeV}, 50 \text{ GeV}]$ .
  - $|\cos\theta_\gamma| < 0.9$ .
  - $M_\gamma \in [75 \text{ GeV}, 100 \text{ GeV}]$ , where Z is everything but the photon.
6. **aa**: Targets  $H \rightarrow \gamma\gamma$ :
  - Has an isolated photon and no isolated leptons.
  - Less than 15 PFOs.
  - $E_H > 125$  GeV.
7. **tau**: Targets  $H \rightarrow \tau^+\tau^-$ :
  - $|\cos\theta_\gamma| < 0.9$ .
  - $E_\gamma > 35$  GeV.
  - Has no isolated leptons.
  - Less than 15 PFOs.
8. **light\_quark**: Targets  $H \rightarrow gg$ :
  - Has no isolated leptons or photons.
  - $btag1 + ctag1 < 0.5$ .
9. **light\_quark2**: Also targets  $H \rightarrow gg$ :
  - Has no isolated leptons or photons.
  - $btag2 + ctag2 < 0.5$ .
10. **isolep1**: Targets  $H \rightarrow W^+W^-, H \rightarrow \tau^+\tau^-$ :
  - Exactly 1 isolated lepton.
11. **isolep2**: Targets  $H \rightarrow W^+W^-, H \rightarrow ZZ^*$ :
  - Exactly 2 isolated leptons.
12. **isolep2**: Targets  $H \rightarrow ZZ^*$ :
  - More than 2 isolated leptons.
13. **isophoton1**: No specific target:
  - Exactly 1 isolated photon.
14. **isophoton\_many**: No specific target:
  - More than 1 isolated photon.
15. **rest**: No specific target:
  - Takes whatever did not belong to any of the previous classes.